Scientific Research Publishing

Open Journal of Microphysics, 2025, 15(2), 25-42
https://www.scirp.org/journal/ojm
ISSN Online: 2162-2469
ISSN Print: 2162-2450

First Principle Study of Spin-Resolved Density of States, Magnetism and Mechanical Properties of the Iron Pnictide Compound $CaFe_2As_2$

Calford Odhiambo Otieno[1], Elijah Omollo Ayieta[2], Mochama Victor Samuel[1*]

[1]Department of Physics, Kisii University, Kisii, Kenya
[2]Department of Physics, University of Nairobi, Nairobi, Kenya
Email: cotieno@kisiiuniversity.ac.ke, ayietaeo@uonbi.ac.ke, mochamavic@gmail.com

How to cite this paper: Otieno, C.O., Ayieta, E.O. and Samuel, M.V. (2025) First Principle Study of Spin-Resolved Density of States, Magnetism and Mechanical Properties of the Iron Pnictide Compound $CaFe_2As_2$. *Open Journal of Microphysics*, **15**, 25-42.
https://doi.org/10.4236/ojm.2025.152002

Received: October 31, 2024
Accepted: March 23, 2025
Published: March 26, 2025

Abstract

We present an *ab-initio* study of the mechanical properties and spin-dependent Density of States (DOS) of the iron pnictide compound $CaFe_2As_2$ at ground state. Ground state energy calculations were performed using Density Functional Theory (DFT) with Projector Augmented Wave (PAW) pseudo potentials and a Plane Wave (PW) basis set. The Generalized Gradient Approximation (GGA) was employed for exchange-correlation effects. The QUANTUM ESPRESSO (QE) code was instrumental in this study, while *THERMO_PW* was utilized to assess mechanical properties. Our results indicate that the compound is mechanically stable. Poisson's ratio suggests that the material is brittle and anisotropic. Electronic structure calculations reveal that $CaFe_2As_2$ exhibits metallic behavior.

Keywords

Iron-Arsenic Compounds, Ferromagnetism, Spin Polarization

1. Introduction

The study of $CaFe_2As_2$, a compound in the family of iron-based superconductors, represents a pivotal focus in condensed matter physics due to the unique properties that iron-pnictide materials exhibit, including high-temperature superconductivity, magnetic ordering and a range of intriguing phase transitions. Discovered in 2008 as part of the larger class of iron-based superconductors, $CaFe_2As_2$ has provided valuable insights into the mechanisms of unconventional supercon-

ductivity, where electron pairing is influenced by magnetic interactions rather than the phonon-mediated pairing seen in traditional superconductors. This has made $CaFe_2As_2$ and related materials a key research area for scientists exploring new pathways for high-temperature superconductivity and its potential applications in energy-efficient technologies and quantum computing.

$CaFe_2As_2$ belongs to the "122" family of iron arsenides, formulated as AFe_2As_2 where *A* represents an alkaline earth metal such as Calcium (Ca), Strontium (Sr), Barium (Ba) or Europium (Eu) [1] [2]. The 122 family of compounds crystallizes in a $ThCr_2Si_2$-type structure with a tetragonal lattice at room temperature [3], in which layers of FeAs alternate with layers of alkaline earth metals. This layered structure is central to the material's behavior, as it supports a quasi-two-dimensional electronic environment where magnetic and electronic interactions are strongly coupled. This lattice structure is also highly adaptable to external influences like pressure and doping, which are known to induce transitions between various structural, magnetic and superconducting phases, making $CaFe_2As_2$ an ideal system for studying the intricate relationship between structure, magnetism and superconductivity.

One of the most defining features of $CaFe_2As_2$ is its magnetic and structural transitions, which occur simultaneously around 170 K under ambient conditions [4]. At this temperature, $CaFe_2As_2$ undergoes a first-order phase transition from a high-temperature paramagnetic tetragonal phase to a low-temperature orthorhombic phase accompanied by antiferromagnetic spin ordering, known as spin-density wave (SDW) ordering. This transition from a paramagnetic to an antiferromagnetic state reflects strong magnetic interactions within the FeAs layers, a characteristic shared among iron-based superconductors, where magnetism is deeply connected to the emergence of superconductivity [5]. The sensitivity of this transition to external pressure and chemical doping highlights the tunable nature of $CaFe_2As_2$ providing a versatile platform for examining how magnetic ordering influences superconducting properties.

An especially intriguing aspect of $CaFe_2As_2$ is the so-called "collapsed tetragonal" phase, which occurs under moderate hydrostatic pressures. In this phase, the lattice structure along the c-axis is significantly compressed, effectively reducing the spacing between FeAs layers and weakening magnetic interactions between the iron atoms [6] [7]. This pressure-induced structural collapse suppresses the antiferromagnetic order and in turn, allows superconductivity to emerge at low temperatures. The ability to induce superconductivity by external pressure rather than chemical alteration sets $CaFe_2As_2$ apart from many other superconducting systems, offering a unique view into the role of lattice structure and magnetism in stabilizing superconducting states.

The electronic structure of $CaFe_2As_2$ is integral to understanding its superconducting properties, as well as its magnetic behavior. The compound's *Fermi surface*, which describes the collection of electronic states at the material's surface, consists of multiple hole and electron pockets primarily associated with Fe 3d or-

bitals. These orbitals, situated within the FeAs layers are responsible for creating quasi-two-dimensional conduction pathways and play a central role in the material's electronic interactions [7] [8]. The *Fermi surface* of $CaFe_2As_2$ is known to exhibit nesting features, where electron and hole pockets align in a way that amplifies magnetic interactions, fostering the spin-density wave (SDW) ordering seen at low temperatures.

When $CaFe_2As_2$ is subjected to external pressure or chemical doping, modifications to the Fermi surface topology directly impact its magnetic and superconducting properties. By altering the electronic band structure, researchers can suppress magnetic ordering, enhance superconducting pairing or even induce new phases. This tunability of the electronic structure and Fermi surface is a hallmark of $CaFe_2As_2$ making it a prime candidate for experiments seeking to unveil the relationship between electronic interactions and superconductivity in iron-based materials.

One of the major areas of interest in the study of $CaFe_2As_2$ is its pressure-induced superconductivity. While $CaFe_2As_2$ does not exhibit superconductivity at ambient pressure, it becomes superconducting at temperatures around 12 K under hydrostatic pressures of approximately 0.4 to 0.8 GPa [1] [8]. This transition is accompanied by the collapse of the tetragonal structure and the suppression of antiferromagnetic ordering, emphasizing how closely superconductivity is tied to structural and magnetic properties in this material. This behavior parallels trends seen in other iron-based superconductors, where external parameters such as pressure or doping tune the magnetic interactions to favor superconductivity.

Chemical doping provides an alternative means of exploring phase transitions in $CaFe_2As_2$. Substituting atoms within the structure such as replacing Ca with other elements (Sr or Ba) or doping Fe sites with transition metals like Co or Ni alters the material's electronic environment and carrier concentration, which can suppress magnetic ordering and promote superconductivity [9] [10]. Studies involving doping highlight the flexibility of $CaFe_2As_2$ in adapting its electronic and magnetic landscape, allowing researchers to probe the effects of electron correlations and lattice changes on its superconducting behavior.

$CaFe_2As_2$ has become a model compound in the study of iron-based superconductors, particularly because of its unique sensitivity to structural, magnetic and electronic modifications. By examining $CaFe_2As_2$, scientists are able to gain insights into the mechanisms that drive high-temperature superconductivity in iron pnictides including the role of magnetic fluctuations, electron correlations and structural transitions. The research findings on $CaFe_2As_2$ contribute significantly to the development of theoretical models describing unconventional superconductivity and may inspire the synthesis of new materials with enhanced superconducting properties.

As the field advances, $CaFe_2As_2$ continues to provide a crucial testing ground for understanding the fundamental physics of superconductivity in iron-based materials. Ongoing studies leveraging advanced experimental techniques such as

neutron scattering, angle-resolved photoemission spectroscopy (ARPES) and muon spin rotation (μSR) along with theoretical approaches like density functional theory (DFT) and dynamical mean-field theory (DMFT), promise to deepen our understanding of this fascinating material and its potential applications in next-generation technologies [11].

2. Computational Methodology

THERMO_PW is a tool used in conjunction with Quantum ESPRESSO for first-principles thermomechanical property calculations based on Density Functional Theory (DFT). It evaluates elastic constants, bulk modulus, Young's modulus, Poisson's ratio and thermal expansion coefficients, which are crucial for understanding mechanical stability in $CaFe_2As_2$.

The program applies small deformations to the equilibrium crystal structure and calculates the resulting stress tensor using DFT. The elastic constants C_{ij} are derived from the linear relation between stress and strain.

$CaFe_2As_2$ undergoes structural and magnetic phase transitions at different temperatures. The thermal expansion coefficient obtained via QHA helps understand how lattice parameters change with temperature, influencing mechanical stability. The tool predicts elastic softening at phase transition temperatures, useful for materials operating at varying conditions.

THERMO_PW can simulate mechanical behavior under hydrostatic pressure, critical for understanding pressure-induced phase transitions in $CaFe_2As_2$. Pressure affects elastic moduli, bond strength and electronic band structure, influencing its superconducting properties.

We utilized Density Functional Theory (DFT) and the QUANTUM ESPRESSO (QE) package to determine the band structure and Density of States (DOS). For mechanical properties, we used THERMO_PW within the QE framework and the Projector Augmented Wave (PAW) for its computational efficiency and systematic convergence, providing accurate results for *ab-initio* electronic structure calculations. *PAW*'s effectiveness is attributed to its scalability and precision in handling complex calculations.

The accuracy and reliability of the computed ground state energy and derived properties (mechanical properties, Spin-resolved density of states (DOS) and magnetism) depend significantly on the choice of PAW pseudopotential and plane-wave (PW) basis set.

The Projected Augmented Wave (PAW) method is a modern pseudopotential approach that improves upon traditional norm-conserving and ultrasoft pseudopotentials by efficiently reconstructing all-electron wavefunctions while maintaining computational efficiency. Handling Transition Metals, PAW is particularly useful for transition metals like Fe, where localized *d* and *f* orbitals play a crucial role in bonding, electronic structure and magnetism. Accurate Description of Core-Valence Interaction, since Ca, Fe and As have strong core-valence interactions, PAW pseudopotentials offer a balance between accuracy and efficiency by

avoiding explicit treatment of core states while capturing their effects on valence states. The PW basis also determines the precision of exchange-correlation effects, which affect the magnetic ground state and spin density distribution.

The PAW method ensures accurate spin polarization, which is critical in capturing the antiferromagnetic (AFM) or paramagnetic (PM) ground state of Fe_2As_2.

On Mechanical Properties PAW improves structural optimization, ensuring precise lattice parameters, bulk modulus and elastic constants, which affect phase stability.

On spin-resolved density of states Density of States (DOS), PAW provides a better description of the Fe *d*-states, crucial in determining the metallic nature of $CaFe_2As_2$.

PAW accurately predicts magnetic moments of Fe atoms, crucial for understanding spin density and *AFM* ordering. Proper PW basis selection refines electronic band structures, ensuring accurate predictions of Fermi surface topology.

The PAW pseudopotential and PW basis set selection play a crucial role in determining the reliability of ground state energy calculations in $CaFe_2As_2$. By ensuring well-converged cutoff energies and k-point sampling, DFT results become more accurate for structural, electronic and magnetic properties, leading to meaningful physical insights into iron-based superconductors.

Our study relies on first-principle computations to analyze electronic orbitals [12] [13], where electrons follow Fermi-Dirac statistics and adhere to the Pauli Exclusion Principle [14] [15]. We use the Born-Oppenheimer approximation to simplify nuclear and electronic structure calculations by treating them at a fixed configuration [16] [17]. Due to the complexity of the electronic Schrödinger equation in systems with many electrons, it is transformed into an algebraic equation and solved numerically [18]. The Hartree-Fock approximation is used to estimate electron behavior by considering each electron moving in an average potential, while post-Hartree-Fock methods account for instantaneous electron correlation effects [15] [19].

3. Results and Discussions

In this section, we report the results obtained from the computational study.

We optimized the cutoff energy and k-points for convergence, achieving optimal values of 45 Ry and 5 Bohr, respectively. The convergence results are illustrated in **Figure 1** and **Figure 2** below.

Lattice optimization refers to finding the equilibrium lattice parameters that minimize the total energy of a crystal structure. In computational studies, these parameters are often unknown or need fine-tuning to match experimental data or theoretical expectations. By finding the lattice parameters that give the lowest possible energy, lattice optimization helps identify the most stable (ground state) crystal structure under specific conditions.

Structural parameters significantly affect a material's electronic, mechanical and optical properties. Optimizing the lattice structure ensures that subsequent

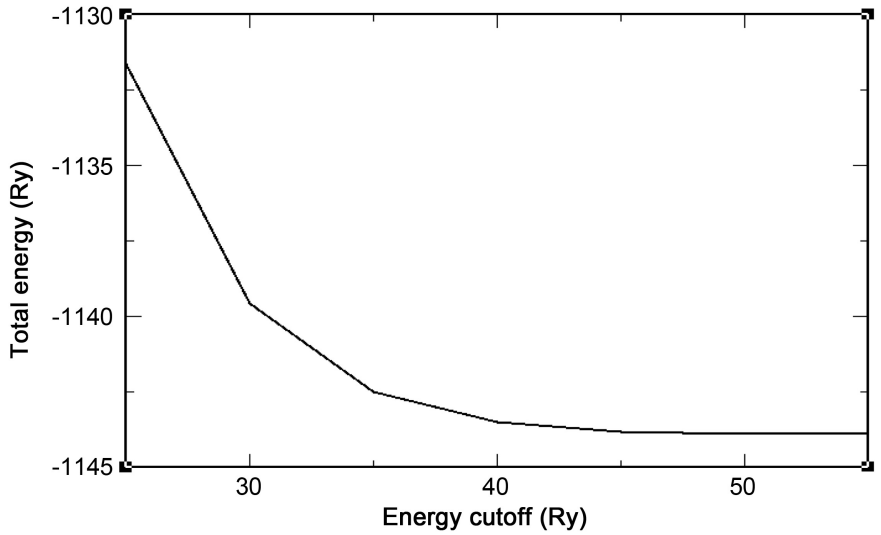

Figure 1. Optimization curve for the energy cut off. Convergence was achieved at 45 Ry.

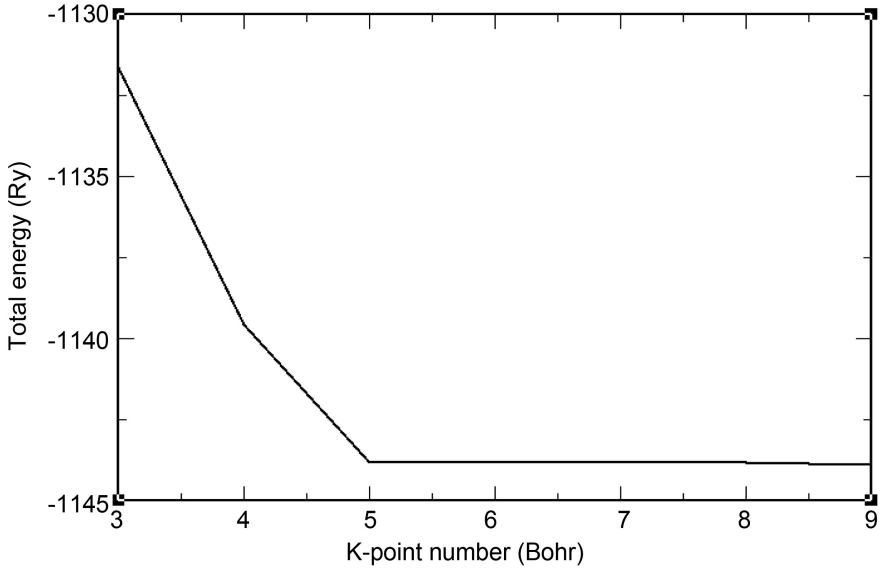

Figure 2. Optimization curve for the k-point. Convergence was achieved at k-point 5.

calculations of properties such as band structure, density of states and mechanical properties are based on a physically realistic model. Incorrect lattice parameters can lead to higher energy structures, which can skew computational predictions and result in errors in derived properties.

Convergence testing ensures that calculated results are stable and accurate relative to certain parameters, reducing errors in predicted material properties. Optimally chosen parameters ensure that calculations are efficient, minimizing computational resources and time. Too high a parameter setting can lead to unnecessarily long computation times without a significant gain in accuracy, while too low a setting can cause inaccurate results.

Both optimized lattice parameters and converged calculation settings lead to

reliable, reproducible results for material properties. For materials with similar structures having an optimized lattice and convergence baseline helps in comparing stability, electronic structure and other properties accurately. Optimized and converged calculations provide data that can be compared directly to experimental measurements, helping validate the computational model.

Together, lattice optimization and convergence testing lay a strong foundation for the computational study of materials, ensuring that the predictions made are meaningful and applicable in real-world contexts.

4. Structural Properties of $CaFe_2As_2$

Calcium iron arsenide ($CaFe_2As_2$) is a member of the iron-based superconductors and crystallizes in a tetragonal structure with the space group 14/mmm [1]. Its structure features alternating layers of FeAs tetrahedra and Ca atoms. In each FeAs layer, iron atoms are surrounded by arsenic atoms in a tetrahedral arrangement, forming a planar network of Fe-As bonds [1]. These layers are interspersed with layers of calcium atoms that sit between the FeAs layers, maintaining the overall crystalline integrity through weak van der Waals interactions. The distinct layered arrangement contributes to the material's electronic properties and superconducting potential. This structure is pivotal in facilitating the electron interactions that can lead to superconductivity under certain conditions [1]. The stable crystal structure is as shown in **Figure 3**.

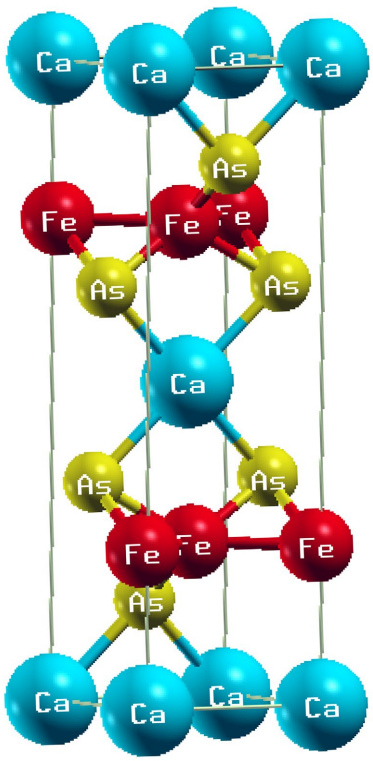

Figure 3. Crystal structure of $CaFe_2As_2$ drawn by quantum espresso Xcrysden package Tetragonal at Stability.

To optimize the lattice constants and cutoff energy for $CaFe_2As_2$ to achieve a stress-free, relaxed structure, we started by selecting an initial crystal structure from experimental data. We then performed density functional theory (DFT) calculations with varying cutoff energies to determine the point at which the total energy converged, typically ensuring accuracy to within 10 - 20 meV/atom. Concurrently, we optimized the lattice constants by allowing both lattice parameters and atomic positions to adjust until the forces on atoms fell below a threshold of 0.01 eV/Å, ensuring minimal stress. Stress tensor components were monitored to confirm that they approached zero, indicating that the structure was in equilibrium. Further validation involved refining the k-point sampling to ensure the results were consistent and converged, providing a final relaxed structure with accurately optimized lattice constants and no residual stress as shown in **Table 1** below.

Table 1. Comparison of experimental and theoretical cell dimensions.

Parameter	This work	Experimental	Reference
$a_0 = b_0$ (ang)	3.249	3.887	[20]
c_0 (ang)	7.493	7.5898	[20]

Theoretical values may be less than experimental values and this is possible because of simplified boundary conditions which sometime oversimplify the system failing to align fully with experimental set up but our optimized cell parameters have a very small margin of error hence in good agreement with both experimental and theoretical work.

The tetragonal crystal structure has six elastic constants as recorded in the **Table 2** below.

Table 2. Elastic constants of $CaFe_2As_2$.

C_{ij}	Value (GPa)
C_{11}	88.86
C_{12}	22.58
C_{13}	28.63
C_{33}	63.51
C_{44}	25.95
C_{66}	31.73

In the context of analyzing the elastic constants of $CaFe_2As_2$, the discussion highlights how the material's response to different types of strain provides insights into its structural rigidity and bond strength. Specifically, the elastic constants C_{12}, C_{13} and C_{44} describe the material's response to uniaxial strain along the [1 0 0], [0 1 0] and [0 0 1] directions. The observation that $C_{11} > C_{33}$ indicates that the crystal

is more rigid in the [1 0 0] and [0 1 0] directions compared to the [0 0 1] direction. This suggests that the *Fe-As* bonds in the planes parallel to the [1 0 0] and [0 1 0] directions are stronger or more resistant to deformation than those in the [0 0 1] direction, reflecting the in-plane bond strength versus the out-of-plane bond strength.

Additionally, the comparison of C_{66} and C_{44} reveals that the shear moduli for the [1 0 0] and [0 0 1] directions are greater than those for the [1 0 0] and [0 1 0] directions. This implies that the material is anisotropic in its resistance to shear deformation in planes aligned with [1 0 0] and [0 0 1] than [1 0 0] and [0 1 0]. Since C_{66} is greater than C_{44}, it implies that the shear deformation in the [1 0 0] - [0 0 1] plane is easier compared to the shear deformation in the [1 0 0] - [0 1 0] plane. This observation underscores the layered nature of the $CaFe_2As_2$ crystal structure, where the in-plane shear responses are more readily accommodated than out-of-plane shear responses, consistent with the weak interlayer interactions compared to the stronger in-plane bonding. This evaluation of the elastic constants thus reinforces the understanding of the material's anisotropic mechanical properties and its layered structural characteristics.

The mechanical stability of a tetragonal crystal structure, such as that of $CaFe_2As_2$, can be effectively assessed using the Born-Huang criteria, which are derived from the general theory of elastic stability [7]. These criteria are based on the elastic constants of the material and ensure that the structure is stable against small perturbations or deformations. For a tetragonal system, the Born-Huang stability criteria are formulated as follows:

1) Stability Conditions:

- $C_{11} > 0$: This condition ensures that the material is stable under uniaxial compression along the [1 0 0] or [0 1 0] directions.
- $C_{33} > 0$: This condition ensures stability under uniaxial compression along the [0 0 1] direction.
- $C_{44} > 0$: This criterion guarantees that the crystal is stable under shear deformation in the [1 0 0] – [0 1 0] plane.
- $C_{66} > 0$: This ensures stability under shear deformation in the [0 0 1] direction.

2) Mechanical Stability Criteria:

- $C_{11} + C_{12} > 0$: This condition ensures that the crystal can sustain small perturbations and does not collapse under applied stresses.
- $C_{11} - C_{12} > 0$: This ensures that the crystal remains stable under uniaxial stress and that the response to such stress is physically plausible.
- $C_{11} + C_{33} - 2C_{13} > 0$: This condition addresses the stability under combined uniaxial stress along different crystallographic directions.

For $CaFe_2As_2$, the application of these criteria involves verifying that the computed elastic constants satisfy the above inequalities. Given that $C_{11} > C_{33}$ and $C_{66} > C_{44}$ were observed, these conditions suggest mechanical stability in the material. Specifically, $C_{11} > C_{33}$ indicates greater rigidity in the in-plane directions compared to the out-of-plane direction, and $C_{66} > C_{44}$ reveals that in-plane shear is easier to

accommodate than out-of-plane shear, reinforcing the layered character of the crystal.

$$C_{ii} > 0 \ (i = 1, 3, 4, 6)$$

$$C_{11} + C_{33} - 2C_{13} > 0$$

$$2(C_{11} + C_{12}) + C_{33} + 4C_{13} > 0$$

$$C_{11} - C_{12} > 0$$

This compound's elastic constants satisfy all of the above mechanical stability conditions. Values of C_{ij} hence can be used in the evaluation of Poisson's and elastic moduli. According to the Voigt approximation criteria, the bulk and shear moduli isotropy can be acquired by linear combination of elastic constants. With a different format, Reuss obtains estimates for bulky and shear moduli isotropy by the use of single crystal elastic constants. Hill confirms that Voigt and Reuss estimates are lower and upper polycrystalline elastic moduli limits, hence the averages became realistic.

$$B = \frac{B_V + B_R}{2} \quad \text{and} \quad G = \frac{G_V + G_R}{2} \quad [21]$$

Young modulus E and Poisson's ratio n in relation to bulky modulus and shear modulus values are tabulated in Table 3 below.

Table 3. Mechanical properties of bulk, shear and Young's modulus and Poisson.

Property	Voigt Approximation	Reuss Approximation	Voigt-Reuss-Hill Average
Bulk modulus (B)	44.55	43.88	44.21
Young modulus (E)	68.39	66.40	67.40
Shear modulus (G)	27.48	26.60	27.04
Poisson ratio (n)	0.24	0.25	0.25

Shear modulus indicates the strength of the material unlike bulk modulus [22]. $G > B$ hence $CaFe_2As_2$ mechanical failure should be corrected by application of the shear component as B represents resistance to fracture. Pugh's ratio determines how ductile or brittle material is [23]. The high value indicates ductility whereas low value indicates brittle nature of the material. For $\frac{B}{G}$ > 1.75 indicates ductility otherwise brittle nature [24]. $\frac{B}{G}$ indicate hardness related inversely whereby the smaller the ratio the harder the material is [1]. For our material $\frac{B}{G}$ < 1.75 confirms brittleness nature. Poisson's ratio (n) assists in the assessment of the mechanical properties of crystalline solids [25]. Its low value indicates stability against shear. Additionally, Poisson's ratio reveals nature of interatomic forces whereby it ranges between 0.25 to 0.50 for central force interaction and outside this range for non-central force interaction [26]. According to Poisson ratio ma-

terials whose ratio is less than 0.26, the material undergoes brittle failure and above this ratio it undergoes ductile failure. Poisson's ratio also reveals brittle nature of $CaFe_2As_2$ Young modulus evaluates resistance against compressive or expansive forces. From our **Table 3** the shear modulus E is small even smaller than that of $BaPb_2As_2$ indicating that $CaFe_2As_2$ obviously cannot withstand large tensile stress.

Cauchy pressure is the difference between C_{12} and C_{44} elastic constants [27]. This parameter reveals more about the elastic response and charge density of solids. Cauchy pressure will indicate ductility or brittleness failure of crystalline solids. A positive or negative Cauchy pressure indicates ductility or brittleness and reveals chemical bonds [27]. Positive value indicates metallic bonds while the negative one indicates covalent bonds. To our study the Cauchy pressure of $CaFe_2As_2$ is negative hence our material is brittle with covalent bonding characteristics.

$CaFe_2As_2$ exhibits strong anisotropy in its structural, mechanical and electronic properties due to its tetragonal crystal symmetry.

Anisotropic materials have direction-dependent properties, that is, their mechanical, thermal and electronic responses vary with orientation. These materials contrast with isotropic materials, where properties remain the same in all directions.

In anisotropic materials, stress-strain responses depend on crystal orientation. In-Plane Direction, strong Fe-As bonds lead to high Young's modulus in this plane. Material resists deformation more strongly than along the c-axis.

Plane Direction, strong Fe-As bonds lead to high Young's modulus in this plane. Material resists deformation more strongly than along the c-axis. Weak interlayer interactions (van der Waals-like forces) cause low stiffness along *c*-axis direction. This results in a lower Young's modulus, higher compressibility and easier deformation.

The shear modulus (G) also varies with direction. If shear stress is applied within the *ab*-plane, resistance is high. If shear stress is applied across layers (*c*-axis shearing), deformation occurs more easily.

On determining whether the material is anisotropic, we made use of the following calculation;

$$A^U = \frac{5G_V}{G_R} + \frac{B_V}{B_R} - 6$$

whereby, if $A^U = 0$ the material would be regarded isotropic. With values drawn from the table above, our calculations indicates that the material is anisotropic with a value of 0.1807 which is in agreement with the studies of the parent compound $ThCr_2Si_2$.

5. Spin Resolved Magnetism

The following is spin-dependent density of states (DOS) and projected density of states of stable tetragonal $CaFe_2As_2$ in the two stripes antiferromagnetic orders in **Figure 4**. The Fe atom contain different crystalline environment for different

magnetic orders and therefore its states are reformed in different ways. The main peaks occupied states are Fe states.

The output file of the Self Consistency Field (scf) calculation gives the lowest energies of the different magnetic orderings of $CaFe_2As_2$. The total energy in the ferromagnetic $CaFe_2As_2$ is −763.50416881 Ry. From this calculation result, it is shown that $CaFe_2As_2$ tetragonal structure at stability is the most stable structure. The negative energy given in the scf output of scf calculation is an indication that a positive work needs to be done to remove an electron from an orbit hence provision of more energy.

The effect of magnetism on the electronic properties of iron pnictide $CaFe_2As_2$ can also be given by the calculated electronic density of states [20]. For the electronic properties, the projected density of states and density of states of tetragonal $CaFe_2As_2$ structure are calculated first by not considering magnetism, that is, magnetization is set at 0.0 Bohr magneton/cell and later by considering magnetization parameter. The spin-polarized total density of states and the projected density of states for the tetragonal $CaFe_2As_2$ were calculated for magnetic configuration 0.0 and 1.0 Bohr magneton/cell. Considering total and absolute magnetization values obtained and plotted in the graphs from the density of states output files as shown in **Figure 4**, it is clearly shown that the spin contributions are exactly the same on either side of the mean position. This indicates that the valence bands which are corresponding to the bonding states are doubly occupied and there is a shift in the magnetization from 0.0 to 1.0 Bohr magneton/cell in the compound [28]. In antiferromagnetism ordering with magnetization 0.0 Bohr magneton/cell, half of the atoms contain magnetization that is opposite to magnetization of the other half and therefore the total magnetization is zero and the contributions of the spins are the same.

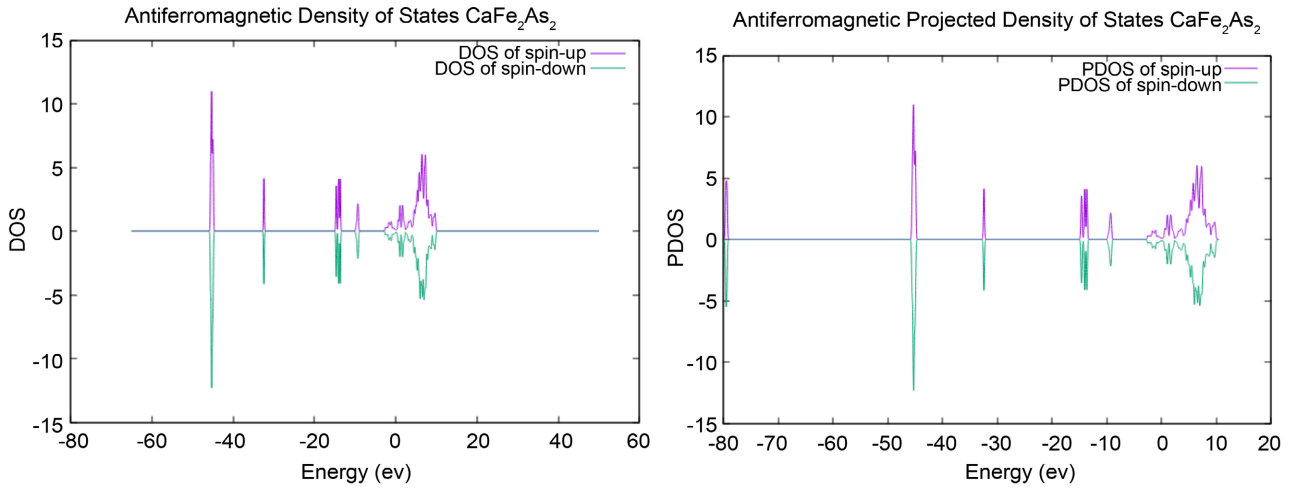

Figure 4. DOS and PDOS of antiferromagnetic $CaFe_2As_2$. Number of electrons with spin-up and spin-down states are the same.

The calculated density of states of ferromagnetic orderings, the spins are oriented parallel to each other minimizing the magnetic energy and the compound

turns into a strong magnet with respect to external application of magnetic field [29]. Consequently, for the antiferromagnetic ordering case, the magnetic energy is minimized when the nearby spins are oriented antiparallel to each other [30]. This is clearly shown by the opposite signs of magnetic interactions to that of ferromagnetic [30] [31].

Figure 4 illustrates the changes in the density of states (DOS) for $CaFe_2As_2$ under ferromagnetic ordering, highlighting a significant difference in the spin populations. In the ferromagnetic state, the system exhibits spin polarization, where one spin channel (typically referred to as "spin-up" or "majority spin") has a significantly larger population than the other ("spin-down" or "minority spin"). This imbalance in spin populations is a hallmark of ferromagnetism [32].

In this ferromagnetic configuration, the DOS for the two spin channels diverges, reflecting that the density of states for each spin is no longer aligned or equivalent [33]. This splitting of the spin-up and spin-down DOS manifests as two distinct features in the DOS plot: one for the majority spin and one for the minority spin. The majority spin channel typically has a higher density of states at the Fermi level compared to the minority spin channel [34].

This spin-dependent DOS splitting results from the exchange interactions characteristic of ferromagnetic materials, which lead to a higher energy density for the majority spin electrons and a lower energy density for the minority spin electrons [35]. Consequently, the Fermi level in the majority spin channel is populated with more available states for conduction, while the minority spin channel may exhibit a reduced density of states or even a gap, depending on the material's specific electronic structure [36].

The lack of alignment between the spin populations in the ferromagnetic state highlights the intrinsic magnetic polarization of the material, which has profound implications for its electronic properties and potential applications. This spin polarization is crucial for spintronic devices, where the ability to control and exploit the spin degree of freedom can lead to enhanced performance and novel functionalities in electronic and magnetic devices [37]. **Figure 5** shows the projected density of states of $CaFe_2As_2$ for spin up and spin down in the ferromagnetic orderings. It is noted that charge density keeps changing from the application of initial magnetization.

From **Figure 5**, it can be observed that the tetragonal $CaFe_2As_2$ exhibits distinct electronic properties depending on its magnetic ordering. In the paramagnetic state, the material displays metallic behavior, as evidenced by the density of states (DOS) starting at the bottom of the valence band and extending up to the Fermi level. This configuration indicates that the valence and conduction bands overlap, allowing for a continuous range of available electronic states at the Fermi level, which facilitates high electrical conductivity due to the abundance of free electrons.

Conversely, when $CaFe_2As_2$ undergoes ferromagnetic ordering, its electronic structure transforms significantly. In this state, the material behaves as a semiconductor. The DOS reveals the presence of a small energy gap between the valence

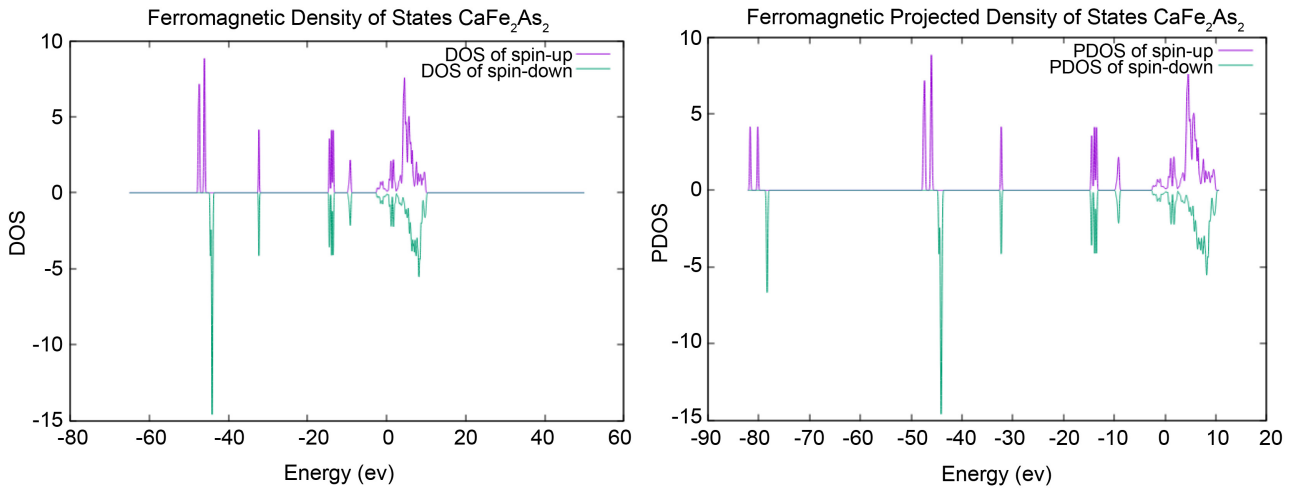

Figure 5. DOS and PDOS Ferromagnetic $CaFe_2As_2$. Number of electrons with spin-up and spin-down states differs.

and conduction bands. This band gap is characterized by the Fermi level lying within it, which indicates a transition from metallic to semiconducting behavior. The small gap implies that while the material can conduct electricity, it does so less efficiently compared to its metallic phase, as fewer electrons are available to participate in conduction.

These observations highlight the impact of magnetic ordering on the electronic properties of $CaFe_2As_2$. In the paramagnetic phase, the overlap of conduction and valence bands supports metallic conductivity. In contrast, the ferromagnetic phase introduces a band gap, transforming the material into a semiconductor with reduced conductivity. This dual behavior underscores the complex interplay between magnetic ordering and electronic structure in $CaFe_2As_2$, offering insights into its potential applications in spintronic devices and magnetic semiconductors.To have a better observation of the effect of magnetization in the projected density of states is plotted for three different magnetic orderings of tetragonal $CaFe_2As_2$.

6. Conclusions

In conclusion, the structural and mechanical analysis of $CaFe_2As_2$ reveals significant insights into its rigidity, bonding characteristics, and magnetic properties. The crystal demonstrates greater rigidity along the [1 0 0] and [0 1 0] directions under uniaxial stress, which highlights the strength of the Fe-As bonds in these planes compared to the [0 0 1] direction. This directional rigidity indicates robust in-plane bonding within the material. However, when considering the material's brittleness, the Poisson ratio, along with the bulk, shear, and Young's moduli, suggests that $CaFe_2As_2$ exhibits brittle behavior, likely due to its covalent bonding characteristics. This is further supported by the negative Cauchy pressure, which indicates that the material's elastic response is consistent with covalent bonding and brittleness.

The convergence of the calculation with a minimum energy value of 45 eV con-

firms the stability and accuracy of our structural model. Additionally, the anisotropy of the material was evaluated by calculating the anisotropy parameter A^U, which indicated isotropy in $CaFe_2As_2$. This isotropy is in alignment with the properties of the parent compound $ThCr_2S_i$, suggesting similar structural behavior and symmetry.

Moreover, the application of a magnetic parameter of 1.0 Bohr magneton per cell reveals that $CaFe_2As_2$ exhibits ferromagnetic properties, predominantly driven by the *Fe* atoms. This magnetic behavior is crucial as it imparts the material with the ability to strongly attract other materials, a property that is highly valuable in various chemical and physical applications. The combined insights into mechanical rigidity, brittleness, isotropy, and ferromagnetic properties make $CaFe_2As_2$ a noteworthy candidate for applications requiring specific mechanical and magnetic functionalities.

Future Research Prospects and Potential Applications of $CaFe_2As_2$

1) High-Temperature Superconductivity Research

Doping Studies: Introducing elements like K, Co, or Ni into $CaFe_2As_2$ may enhance superconducting transition temperatures by modifying band filling and Fermi surface nesting.

Pressure-Induced Superconductivity: Investigating quantum phase transitions under pressure could reveal new high-temperature superconducting states.

Electron-Phonon and Spin-Fluctuation Interactions: Further studies on phonon-mediated pairing and spin-fluctuation-driven superconductivity could provide insights into unconventional pairing mechanisms.

2) Application in Electronic and Magnetic Devices

Magneto-Resistance Devices: The tunable magnetic structure of $CaFe_2As_2$ can be useful in spintronic applications, where control over magnetization and DOS can be exploited.

Acknowledgements

We gratefully acknowledge the computational resources and support provided by the Center for High Performance Computing (CHPC). Their advanced computing infrastructure was essential for the successful execution of the computational work required for this study. Without their resources and technical assistance, achieving the detailed and accurate results presented here would not have been possible.

Conflicts of Interest

The authors declare no conflicts of interest regarding the publication of this paper.

References

[1] Samuel, M.V., Otieno, C.O. and Nyawere, P. (2023) Density Functional Study of Mechanical, Electronic and Pressure Induced Phase Transition Properties of $CaFe_2As_2$.

Open Journal of Microphysics, **13**, 36-51.
https://doi.org/10.4236/ojm.2023.133004

[2] Omboga, N.K. and Otieno, C.O. (2020) Structural and Electronic Properties of the Iron Pnictide Compound $EuFe_2As_2$ from First Principles. *Journal of Physics Communications*, **4**, Article ID: 025007. https://doi.org/10.1088/2399-6528/ab5bb0

[3] Felner, I. (2001) The Interrelation between Magnetism and Superconductivity in RNi_2B_2C: The Mössbauer Effect. In: Müller, K.H. and Narozhnyi, V., Eds., *Rare Earth Transition Metal Borocarbides* (*Nitrides*): *Superconducting, Magnetic and Normal State Properties*, Springer, 197-210. https://doi.org/10.1007/978-94-010-0763-4_21

[4] Canfield, P.C., Bud'ko, S.L., Ni, N., Kreyssig, A., Goldman, A.I., McQueeney, R.J., *et al.* (2009) Structural, Magnetic and Superconducting Phase Transitions in Cafe2as2 under Ambient and Applied Pressure. *Physica C*: *Superconductivity*, **469**, 404-412. https://doi.org/10.1016/j.physc.2009.03.033

[5] Niedziela, J.L., Sanjeewa, L.D., Podlesnyak, A.A., DeBeer-Schmitt, L., Kuhn, S.J., de la Cruz, C., *et al.* (2021) Magnetoelastic Coupling, Negative Thermal Expansion, and Two-Dimensional Magnetic Excitations in Feas. *Physical Review B*, **103**, Article ID: 094431. https://doi.org/10.1103/physrevb.103.094431

[6] Yildirim, T. (2009) Frustrated Magnetic Interactions, Giant Magneto-Elastic Coupling, and Magnetic Phonons in Iron-Pnictides. *Physica C*: *Superconductivity*, **469**, 425-441. https://doi.org/10.1016/j.physc.2009.03.038

[7] Omboga, N.K., Otieno, C.O. and Nyawere, P.W.O. (2020) First Principle Study of the Mechanical Properties and Phonon Dispersion of the Iron Pnictide Compound $EuFe_2As_2$. *The Scientific World Journal*, **2020**, Article ID: 5986073. https://doi.org/10.1155/2020/5986073

[8] Drye, T. (2014) Structural Changes and the Nature of Superconductivity in Rare-Earth Doped $CaFe_2As_2$. University of Maryland.

[9] Shibin, T. (2020) Structural and Electrochemical Characterisation of Transition Metal Doped Perovskite Related Structure ABO3-δ (A= Ca/Sr/Ba; B= Fe/Si/In). https://www.proquest.com/open-view/d6702b427dbab1d7cea4a6031df1f4d2/1?cbl=18750&pq-origsite=gscholar

[10] Munazat, D.R., Kurniawan, B., Kurita, N., Wang, X., Manawan, M.T.E., Sudiro, T., *et al.* (2024) Investigation of the Impact of A-Site Cation Disorder on the Structure, Magnetic Properties, and Magnetic Entropy Change of Trisubstituted Divalent Ions in $La_{0.7}(Ba, Ca, Sr)_{0.3}MnO_3$ Manganite. *Physical Chemistry Chemical Physics*, **26**, 18343-18367. https://doi.org/10.1039/d4cp01039f

[11] Tranquada, J.M. (2020) Cuprate Superconductors as Viewed through a Striped Lens. *Advances in Physics*, **69**, 437-509. https://doi.org/10.1080/00018732.2021.1935698

[12] Martinez, T.J. and Levine, R.D. (1996) First-Principles Molecular Dynamics on Multiple Electronic States: A Case Study of Nai. *The Journal of Chemical Physics*, **105**, 6334-6341. https://doi.org/10.1063/1.472486

[13] Otieno, O.V., Ongwen, N. and Otieno, C. (2024) Tuning the Structural and Mechanical Properties of Sic-Li and Sic-Na Alloys for Aerospace Application: An *ab Initio* Study. *Journal of Physics Communications*, **8**, Article ID: 115001. https://doi.org/10.1088/2399-6528/ad756f

[14] Pauli, W. (1924) Zur Frage der theoretischen Deutung der Satelliten einiger Spektrallinien und ihrer Beeinflussung durch magnetische Felder. *Naturwissenschaften*, **12**, 741-743. https://doi.org/10.1007/bf01504828

[15] Agora, J.O., Otieno, C., Nyawere, P.W.O. and Manyali, G.S. (2022) Elastic Behavior,

Pressure-Induced Doping and Superconducting Transition Temperature of $GdBa_2Cu_3O_{7-x}$. *Journal of Physics Communications*, **6**, Article ID: 015004. https://doi.org/10.1088/2399-6528/ac438c

[16] Agostini, F. and Curchod, B.F.E. (2022) Chemistry without the Born-Oppenheimer Approximation. *Philosophical Transactions of the Royal Society A*: *Mathematical, Physical and Engineering Sciences*, **380**, Article ID: 20200375. https://doi.org/10.1098/rsta.2020.0375

[17] Agora, J.O., Otieno, C., Nyawere, P.W.O. and Manyali, G.S. (2020) Ab Initio Study of Pressure Induced Phase Transition, Structural and Electronic Structure Properties of Superconducting Perovskite Compound $GdBa_2Cu_3O_{7-x}$. *Computational Condensed Matter*, **23**, e00461. https://doi.org/10.1016/j.cocom.2020.e00461

[18] Jomo, P.O., Otieno, C.O. and Nyawere, P.W.O. (2020) *Ab Initio* High-Pressure Study of Semiconductor-Metal Phase Transition of the Chalcogenide Compound $KPSe_6$. *Advances in Condensed Matter Physics*, **2020**, Article ID: 3407141. https://doi.org/10.1155/2020/3407141

[19] Slater, J.C. (1951) A Simplification of the Hartree-Fock Method. *Physical Review*, **81**, 385-390. https://doi.org/10.1103/physrev.81.385

[20] Ronning, F., Klimczuk, T., Bauer, E.D., Volz, H. and Thompson, J.D. (2008) Synthesis and Properties of $CaFe_2As_2$ Single Crystals. *Journal of Physics*: *Condensed Matter*, **20**, Article ID: 322201. https://doi.org/10.1088/0953-8984/20/32/322201

[21] Parvin, F. and Naqib, S.H. (2019) Structural, Elastic, Electronic, Thermodynamic, and Optical Properties of Layered $BaPd_2As_2$ Pnictide Superconductor: A First Principles Investigation. *Journal of Alloys and Compounds*, **780**, 452-460. https://doi.org/10.1016/j.jallcom.2018.12.021

[22] Anderson, D. and Stokoe, K. (1978) Shear Modulus: A Time-Dependent Soil Property. In: Silver, M.L. and Tiedemann, D., Eds., *Dynamic Geotechnical Testing*, ASTM International, 66-90. https://doi.org/10.1520/stp35672s

[23] Thompson, R.P. and Clegg, W.J. (2018) Predicting Whether a Material Is Ductile or Brittle. *Current Opinion in Solid State and Materials Science*, **22**, 100-108. https://doi.org/10.1016/j.cossms.2018.04.001

[24] Pan, Y. and Guan, W.M. (2017) Probing the Balance between Ductility and Strength: Transition Metal Silicides. *Physical Chemistry Chemical Physics*, **19**, 19427-19433. https://doi.org/10.1039/c7cp03182c

[25] Cho, S., Chasiotis, I., Friedmann, T.A. and Sullivan, J.P. (2005) Young's Modulus, Poisson's Ratio and Failure Properties of Tetrahedral Amorphous Diamond-Like Carbon for MEMS Devices. *Journal of Micromechanics and Microengineering*, **15**, 728-735. https://doi.org/10.1088/0960-1317/15/4/009

[26] Greaves, G.N. (2012) Poisson's Ratio over Two Centuries: Challenging Hypotheses. *Notes and Records*: *the Royal Society Journal of the History of Science*, **67**, 37-58. https://doi.org/10.1098/rsnr.2012.0021

[27] Milstein, F. and Rasky, D.J. (1985) Theoretical Expression, $C_{44}= 13(2C_{11} - C_{12})$ in Better Agreement with Experiment than the Cauchy Relation C44 = C12 for F.c.c. Crystals. *Solid State Communications*, **55**, 729-732. https://doi.org/10.1016/0038-1098(85)90244-3

[28] Sapkota, A. (2018) Studies of Spin Dynamics in 122 Transition metal Arsenides Using Inelastic Neutron Scattering Technique. Iowa State University. https://www.proquest.com/open-view/2bc552f14ae8aa944ae4100127db400a/1?cbl=18750&pq-origsite=gscholar

[29] Korenblit, I.Y. and Shender, E.F. (1978) Ferromagnetism of disordered systems. *Soviet Physics Uspekhi*, **21**, 832-851. https://doi.org/10.1070/pu1978v021n10abeh005686

[30] Roth, W.L. (1958) Multispin Axis Structures for Antiferromagnets. *Physical Review*, **111**, 772-781. https://doi.org/10.1103/physrev.111.772

[31] Keffer, F. and O'Sullivan, W. (1957) Problem of Spin Arrangements in MnO and Similar Antiferromagnets. *Physical Review*, **108**, 637-644. https://doi.org/10.1103/physrev.108.637

[32] Lyons, T.P., Gillard, D., Molina-Sánchez, A., Misra, A., Withers, F., Keatley, P.S., *et al.* (2020) Interplay between Spin Proximity Effect and Charge-Dependent Exciton Dynamics in $MoSe_2$/$CrBr_3$ van der Waals heterostructures. *Nature Communications*, **11**, Article No. 6021. https://doi.org/10.1038/s41467-020-19816-4

[33] Zhang, X. and Butler, W.H. (2004) Large Magnetoresistance in bcc Co/MgO/Co and FeCo/MgO/FeCo Tunnel Junctions. *Physical Review B*, **70**, Article ID: 172407. https://doi.org/10.1103/physrevb.70.172407

[34] Butler, W.H., Zhang, X., Schulthess, T.C. and MacLaren, J.M. (2001) Spin-Dependent Tunneling Conductance of Fe|MgO|Fe Sandwiches. *Physical Review B*, **63**, Article ID: 054416. https://doi.org/10.1103/physrevb.63.054416

[35] Janas, D.M., Droghetti, A., Ponzoni, S., Cojocariu, I., Jugovac, M., Feyer, V., *et al.* (2022) Enhancing Electron Correlation at a 3D Ferromagnetic Surface. *Advanced Materials*, **35**, Article ID: 2205698. https://doi.org/10.1002/adma.202205698

[36] Bibes, M., Villegas, J.E. and Barthélémy, A. (2011) Ultrathin Oxide Films and Interfaces for Electronics and Spintronics. *Advances in Physics*, **60**, 5-84. https://doi.org/10.1080/00018732.2010.534865

[37] Zhao, X.G., Richardson, W.H., Chen, J., Li, J., Noodleman, L., Tsai, H., *et al.* (1997) Density Functional Calculations of Electronic Structure, Charge Distribution, and Spin Coupling in Manganese-Oxo Dimer Complexes. *Inorganic Chemistry*, **36**, 1198-1217. https://doi.org/10.1021/ic9514307